

Babinet's principle for optical frequency metamaterials and nanoantennas

T. Zentgraf,* T. P. Meyrath, A. Seidel, S. Kaiser, and H. Giessen

4. Physikalisches Institut, Universität Stuttgart, Pfaffenwaldring 57, D-70550 Stuttgart, Germany

C. Rockstuhl and F. Lederer

Institut für Festkörpertheorie und -optik, Friedrich-Schiller-Universität Jena, Max-Wien Platz 1, D-07743 Jena, Germany

(Received 4 June 2007; published 10 July 2007)

We consider Babinet's principle for metamaterials at optical frequencies and include realistic conditions which deviate from the theoretical assumptions of the classic principle such as an infinitely thin and perfectly conducting metal layer. It is shown that Babinet's principle associates not only transmission and reflection between a structure and its complement but also the field modal profiles of the electromagnetic resonances as well as effective material parameters—a critical concept for metamaterials. Also playing an important role in antenna design, Babinet's principle is particularly interesting to consider in this case where the metasurfaces and their complements can be regarded as variations on a folded dipole antenna array and patch antenna array, respectively.

DOI: 10.1103/PhysRevB.76.033407

PACS number(s): 78.20.Ci, 41.20.Jb, 73.20.Mf, 75.30.Kz

Babinet's principle is a classic concept of the wave theory of light. It had originally been used to simplify the analysis of certain diffraction problems.¹ In scalar formulation, Babinet's principle yields a correspondence between an amplitude transmission mask and a complementary mask. Beyond this original application, Babinet's principle has found great importance in, for example, the design of broadband antennas. In such designs, ideally, it is possible to produce antennas which have an arbitrarily large bandwidth. This can involve the use of an antenna form which has a conductor pattern that is itself its own complement.² Another important application has been in the formation of frequency-selective surfaces in the far infrared. This has involved the use of grid structures and their complementary structures which can be seen as capacitive and inductive gratings, respectively.³ Most of these applications are designed to operate at microwave frequencies where metals can be regarded as near-perfect conductors. Perfect conductivity is a mandatory requisite to apply Babinet's principle in a rigorous manner.¹ With few exceptions (e.g., Ref. 4), Babinet's principle is traditionally applied to amplitude transmission structures while neglecting the presence of resonant eigenmodes. Localized eigenmodes contribute to the optical properties of a wide variety of nano- and micro-optical devices, such as subwavelength apertures, optical antennas, or materials with novel electromagnetic properties.

These novel properties have become available with the development of metamaterials composed of resonant unit cells.⁵ In the microwave domain, one of the most common designs for such a unit cell is the split ring resonator (SRR).⁶ By scaling down the size of SRRs, it is possible to shift the frequency of the fundamental eigenmodes of the SRRs into the optical range.⁷ It has thus far been unclear whether Babinet's principle is applicable to such conductor patterns in optical metamaterials. Because a metamaterial is generally to be considered an effective medium, the structures are ideally much smaller than the wavelength of incident light. In typical optical metamaterial regimes, normal metal boundary conditions are not entirely applicable because the field penetration depth is comparable to the structure size. Addition-

ally, all metamaterials which have been realized thus far have suffered from relatively high losses, especially in the optical region. This leads to the question as to whether Babinet's principle can even be applied.

These questions demand answers because Babinet's principle is a fundamental concept in optics as well as in radio and microwave frequency antenna physics. With recent progress in optical frequency antennas⁸ and metamaterials, the opportunity of using Babinet's principle to explore new metamaterial designs and possibilities for these systems is desirable. An ideal test bed to answer these questions is to consider the conductor patterns of an SRR and a complementary SRR (C-SRR) as shown in Fig. 1. SRR structures are explored here because they have been crucial in the development of metamaterials and are well understood in the microwave and optical⁹ domains. Recent work has been performed with these structures in the microwave¹⁰ and terahertz¹¹ regions, where the used copper and gold as SRR material represents a nearly perfect conductor. Meanwhile, it was shown that the C-SRR structures can help in the design of narrow band frequency-selective structures with microstrip technology.¹² Additionally, these patterns correspond to important antenna structures. This is apparent when regarding the single SRR in Fig. 1(a) as a folded dipole antenna, whereas the complementary structure in Fig. 1(b) can be re-

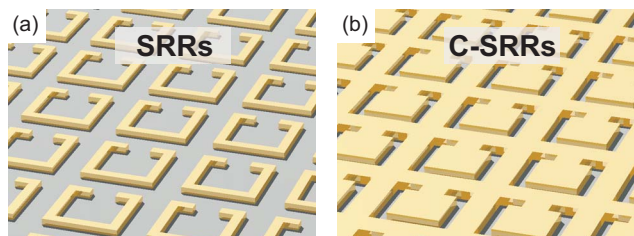


FIG. 1. (Color online) Schematic view of (a) the fabricated gold SRRs and (b) their complementary structure. Both structures have a height of 15 nm and are deposited on a 2-mm-thick Infrasil glass substrate.

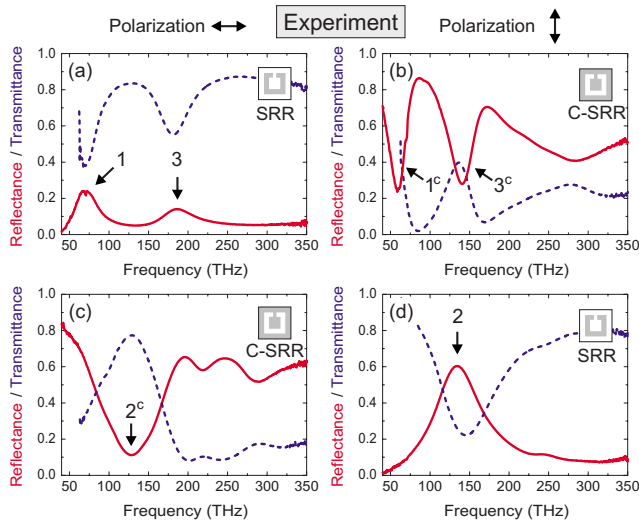


FIG. 2. (Color online) Measured transmittance (blue, dotted) and reflectance (red, solid) of [(a) and (d)] SRRs and [(b) and (c)] C-SRRs for the two polarization configurations. The numbers mark the eigenmodes described in the text.

garded as a variation of a planar patch antennas. Both have important applications in microwave physics.²

In this Brief Report, we establish that it is indeed possible to utilize Babinet's principle for metamaterials in the optical domain when the system is nonideal. If a complementary wave with $\mathbf{E}_0^c = c\mathbf{B}_0$ and $\mathbf{B}_0^c = -\mathbf{E}_0/c$ illuminates a complementary screen S^c , the full vectorial Babinet's principle states that the total scattered fields behind the screen must satisfy $\mathbf{E} - c\mathbf{B}^c = \mathbf{E}_0$ and $\mathbf{B} - \mathbf{E}^c/c = \mathbf{B}_0$.¹³ Here, \mathbf{E}_0 and \mathbf{B}_0 are the incident fields from the original screen S . Although this principle is only exact for a perfectly conducting thin planar screen of infinite extent, we consider its validity for the optical metamaterial regime. Since metamaterials are composed of subwavelength structures, only the zeroth diffraction order can propagate. On the other hand, metamaterials have intrinsic resonances.⁹ An approach to the interpretation of Babinet's principle is necessary, which considers the electric and magnetic fields due to these resonances. The complementary nature of these fields is discussed below.

Figure 1 schematically shows arrays of periodically arranged gold SRR and C-SRR structures. Both types of structures were fabricated on top of a glass substrate (Infrasil, $n = 1.46$) using electron beam lithography techniques. The SRRs and C-SRRs have outer dimensions (as confirmed by electron microscopy) of $420 \times 420 \text{ nm}^2$ with line and slit widths of 60 nm and 70 nm, respectively. The size of the gap is 220 nm for the SRR and 240 nm for the C-SRR. The height of the gold layer in both cases is 15 nm.

The optical response of the samples was measured over a wide frequency range with a Fourier transform infrared spectrometer. Figure 2 shows the measured transmittance and reflectance spectra of the SRR and C-SRR structures for both polarization directions. Due to the incipient strong absorption of the glass substrate below 70 THz, values for the reflectance are only attainable for the low frequency edge of the measured spectra. For the SRR, three pronounced resonances appear in the spectra, two for the polarization parallel

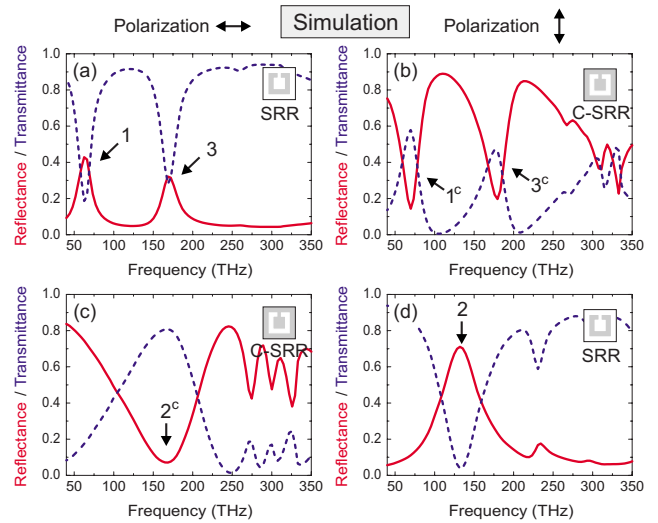


FIG. 3. (Color online) Calculated transmittance (blue, dotted) and reflectance (red, solid) of [(a) and (d)] SRRs and [(b) and (c)] C-SRRs for the two polarization configurations. The numbers mark the eigenmodes described in the text.

to the gap of the SRRs and one for the polarization perpendicular to the gap. These are the first three lowest-order plasmonic eigenmodes of the SRR.⁹ These modes are labeled on the plot by the number of nodes of the electric field component normal to the plane of the SRR. The fundamental mode near 70 THz, for instance, is indicated by "1". This mode plays a particularly important role in the magnetic dipolar response of the SRR if the magnetic field component of the incident light field is oriented perpendicular to the SRR plane.⁷

When comparing the spectral response of the SRRs with that of the complementary structures [Figs. 2(b) and 2(c)], it is obvious that the behavior of the reflectance has been interchanged with the transmittance when the polarization direction of the light is rotated by 90°. Each peak in the reflectance of the SRRs corresponds to a peak in the transmittance of the C-SRRs. The slight shift in the spectral peak positions is due to deviations of the fabricated structure sizes between the SRRs and the C-SRRs; this leads to small differences in resonance frequencies. Although gold already shows a strong absorption in this frequency region, the peaks (dips) in the transmittance (reflectance) of the complementary structure are well pronounced. Even the spectral width of the modes is comparable to the eigenmodes of the SRR structure.

For a rigorous simulation of the scattering response, a technique based on the Fourier modal method¹⁴ was employed which, for the description of the material, used the dielectric function of gold from Ref. 15. The results of the simulated spectra are shown in Fig. 3. For the calculation, the structure sizes of the fabricated SRRs and C-SRRs were taken into account. For high frequencies, particularly above 300 THz, the measured peaks in the spectra of the C-SRRs are less pronounced in comparison to those calculated and seem to be strongly broadened. Further experiments with the same structure sizes for the C-SRRs but different periods show that these peaks shift noticeably to lower frequencies in the spectrum when the distance between sites is increased.

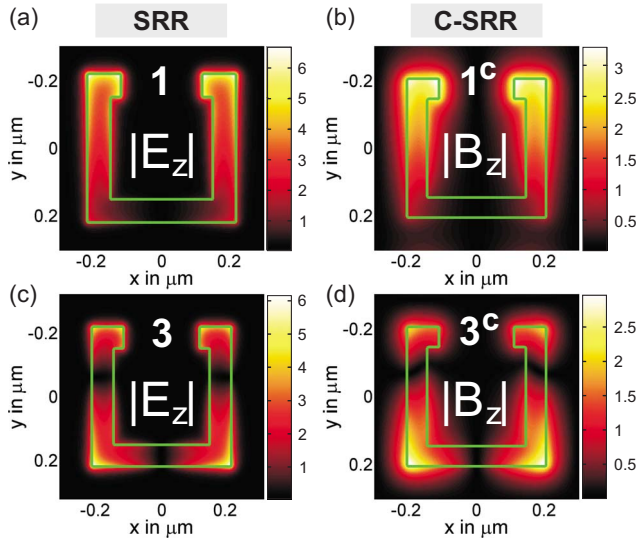


FIG. 4. (Color online) Calculated field distribution for the first- and third-order eigenmodes of the [(a) and (c)] SRR and [(b) and (d)] C-SRR. The plot shows the field component ($|E_z|$ and $|B_z|$) normal to the structure plane 7.5 nm above the surface. The fields are normalized to the illuminating electric and magnetic fields, respectively.

This behavior is a typical sign for the excitation of propagating surface plasmons in the metallic film by the periodicity¹⁶ and will not be considered here further.

To understand the excited modes in the case of the C-SRRs better, the near-field distributions of the first and third resonance [indicated by 1 (1^c) and 3 (3^c) in Fig. 3] were calculated for both cases. The calculations were performed with the finite difference time domain method. The results for the component of the electric and magnetic fields normal to the surface are shown in Fig. 4. For the SRR resonance 1, the electric field component E_z (normal to the plane of the paper) shows a strong enhancement at the two ends of the ring structure. As recently shown, this characterizes the first-order eigenmode of the SRR due to the excitation of a fundamental localized plasmon mode along the entire ring.⁹

In the case of the complementary structure, Babinet's principle anticipates that each electric field component \mathbf{E} should be interchanged with its magnetic counterpart \mathbf{B} . The magnetic near field, therefore, exhibits the analogous behavior in the C-SRR, as shown in Fig. 4(b). This magnetic field distribution shows qualitatively the same behavior as the electric field for the first-order eigenmode of the SRR. In analogy to the SRR eigenmodes, higher-order modes of the C-SRR also occur (field distributions are only shown for the first- and third-order resonances in Fig. 4). Therefore, it is reasonable to use an analogous labeling scheme for the C-SRR eigenmodes as for those of the SRR—labeling in accordance to the node number of the appropriate field in z direction. In a microscopic picture, the eigenmodes of the SRR are related to the excitation of localized surface plasmon polaritons in the metallic nanoring, whereas the eigenmodes of the C-SRR are related to localized guided modes in the nanoslits through the metal film.

These localized guided modes show the same behavior as

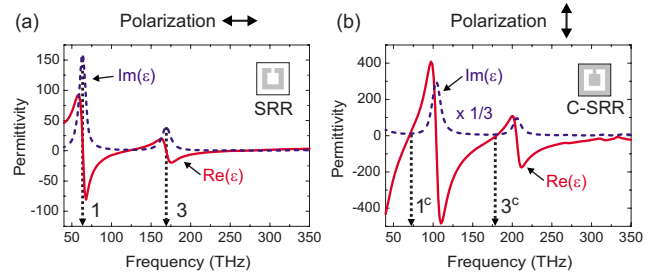


FIG. 5. (Color online) Retrieved real part (solid line) and imaginary part (dotted line) for the permittivity of the SRR and C-SRR slab structures from the calculated spectra. The vertical dotted lines together with the numbers mark the transmission and/or reflection resonance positions in the spectra. $\text{Im}(\epsilon)$ in (b) is shown with a 1/3 magnitude scale.

modes in nanocavities. The light is guided as eigenmodes inside the slits and can propagate through the metal film with relatively low losses. As for the excitation of the eigenmodes of the SRR, the resonance position in the spectrum of such cavity modes is determined mainly by the geometric details of the structure. Because the SRR and C-SRR structures are of subwavelength size, a macroscopic picture involving effective material parameters¹⁷ can be used. In this picture, efficient transmission of light through a nanostructured metal film can be intuitively understood. This requires the extraction of an effective relative permittivity ϵ and permeability μ .

In addition to the complementary relationships between the SRR and C-SRR structures which we have already discussed, we find a complementary relationship in effective permittivity resonances. This relationship gives a correspondence between the spectral positions of the plasmonic eigenmodes and the positions of effective material resonances. The peaks or dips in the reflectance and transmittance spectra indicate the plasmonic eigenmodes. On the other hand, effective material resonances appear in the permittivity ϵ , shown in Fig. 5. The permittivity was retrieved from the simulated spectra of Figs. 3(a) and 3(b). Due to the propagation of the light perpendicular to the SRR plane, only a resonant behavior in the permittivity occurs, and the permeability (not shown) is nearly unresponsive ($\mu \approx 1$). In Fig. 5, the labeled vertical lines show the spectral locations of the indicated plasmonic eigenmodes from Fig. 3.

When comparing the spectra of the SRRs with the retrieved permittivity [Fig. 5(a)], we see that the spectral positions of the plasmonic eigenmodes coincide with the maximum of the imaginary part of the permittivity. The plasmonic resonances, therefore, spectrally coincide with the resonances in the effective material parameters.

In the case of the C-SRR structures shown in Fig. 5(b), the locations of resonances in ϵ have a complementary relationship with the plasmonic resonance positions. Rather than being located at the same spectral positions, the plasmonic resonances (high transmission) correspond to spectral locations where $\text{Re}(\epsilon)$ is near unity. The locations of the ϵ resonances, therefore, correspond to regions far from the plasmonic resonances and are thus broad sections of high reflectivity.

This is explicable in light of the fact that the material layer with effective ϵ near unity is well matched to its environment (i.e., air, glass). In such a case, high transmission is expected. This interpretation is also consistent in the SRR case, in which locations with $\text{Re}(\epsilon)$ near unity correspond to broad regions of high transmission. This behavior is complementary between SRR and C-SRR and can be regarded as *Babinet's principle for effective material parameters in metamaterials*. Because the effective material resonances occur far from the resonances in the reflectance and/or transmittance spectra, this aspect is of particular interest for metamaterials. This approach connects the guided mode picture and the effective material picture and illustrates complete correspondence between the pair of subwavelength structures. This high transmission and impedance-matched behavior is especially useful in the designs of enhanced transmission subwavelength structures as well as in efficient nanoantennas.^{8,18}

In conclusion, we have shown that Babinet's principle qualitatively holds for metamaterials at near-infrared optical frequencies, despite the fact that the properties of the system

include subwavelength structures and lack perfect conductivity and ideal boundary conditions. With the example of the well-known SRR, we have demonstrated that, for a complementary structure (C-SRR) illuminated by a complementary wave, the reflection and transmission can be interchanged. The eigenmodes of the C-SRR can be denoted in analogy to the eigenmodes of the SRR; this analogy is an implication of Babinet's principle. We have shown that there is additionally a complementary behavior of effective material parameters. Babinet's principle, therefore, can open possibilities for the design and understanding of metamaterials, metasurfaces, and nanoantennas in the optical domain, as it has done for radio frequency and microwave antenna physics.

Our work was supported by the Federal Ministry of Education and Research (Grant No. 13N9155) and the Deutsche Forschungsgemeinschaft (Grant No. FOR557). T.P.M. and T.Z. thank the Alexander von Humboldt Foundation and the Landesstiftung Baden-Württemberg, respectively. Some computations utilized the IBM p690 cluster (JUMP) of the Forschungszentrum in Jülich, Germany.

*Also at Max-Planck-Institut für Festkörperforschung, Heisenbergstrasse 1, D-70569 Stuttgart, Germany.

¹M. Born and E. Wolf, *Principles of Optics* (Cambridge University Press, Cambridge, 2002).

²T. Lee, *Planar Microwave Engineering* (Cambridge University Press, Cambridge, 2004).

³R. Ulrich, *Infrared Phys.* **7**, 37 (1967).

⁴D. H. Dawes, R. C. McPhedran, and L. B. Whitbourn, *Appl. Opt.* **28**, 3498 (1989).

⁵S. A. Ramakrishna, *Rep. Prog. Phys.* **68**, 449 (2005).

⁶J. B. Pendry, A. J. Holden, D. J. Robbins, and W. J. Stewart, *IEEE Trans. Microwave Theory Tech.* **47**, 2075 (1999).

⁷S. Linden, C. Enkrich, M. Wegener, J. Zhou, T. Koschny, and C. M. Soukoulis, *Science* **306**, 1351 (2004).

⁸P. Mühlischlegel, H.-J. Eisler, O. J. F. Martin, B. Hecht, and D. W. Pohl, *Science* **308**, 1607 (2005).

⁹C. Rockstuhl, F. Lederer, C. Etrich, T. Zentgraf, J. Kuhl, and H. Giessen, *Opt. Express* **14**, 8827 (2006).

¹⁰F. Falcone, T. Lopetegui, M. A. G. Laso, J. D. Baena, J. Bonache,

M. Beruete, R. Marqués, F. Martín, and M. Sorolla, *Phys. Rev. Lett.* **93**, 197401 (2004).

¹¹H.-T. Chen, J. F. O'Hara, A. J. Taylor, R. D. Averitt, C. Highstrete, M. Lee, and W. J. Padilla, *Opt. Express* **15**, 1084 (2007).

¹²J. Bonache, F. Martín, F. Falcone, J. D. Baena, T. Lopetegui, J. García-García, M. A. G. Laso, I. Gil, A. Marcotegui, R. Marqués, and M. Sorolla, *Microwave Opt. Technol. Lett.* **46**, 508 (2005).

¹³J. D. Jackson, *Classical Electrodynamics* (Wiley, New York, 1999).

¹⁴L. Li, *J. Opt. Soc. Am. A* **14**, 2758 (1997).

¹⁵P. B. Johnson and R. W. Christy, *Phys. Rev. B* **6**, 4370 (1972).

¹⁶W. L. Barnes, A. Dereux, and T. W. Ebbesen, *Nature (London)* **424**, 824 (2003).

¹⁷D. R. Smith, S. Schultz, P. Markoš, and C. M. Soukoulis, *Phys. Rev. B* **65**, 195104 (2002).

¹⁸T. W. Ebbesen, H. J. Lezec, H. F. Ghaemi, T. Thio, and P. A. Wolff, *Nature (London)* **391**, 667 (1998).